C. R. Chimie 15 (2012) 511–516

Contents lists available at SciVerse ScienceDirect

Comptes Rendus Chimie

www.sciencedirect.com

Preliminary communication/Communication

Room-temperature sulfidation of copper nanoparticles with sulfur yielding covellite nanoparticles

Markéta Urbanová [a], Jaroslav Kupčík [a,b], Petr Bezdička [b], Jan Šubrt [b], Josef Pola [a,*]

[a] Laboratory of Laser Chemistry, Institute of Chemical Process Fundamentals, ASCR, 16502 Prague, Czech Republic
[b] Institute of Inorganic Chemistry, ASCR, 25068 Řež, Czech Republic

ARTICLE INFO

Article history:
Received 7 October 2011
Accepted after revision 27 March 2012
Available online 22 May 2012

Keywords:
Cu nanoparticles
Elemental sulfur
Room-temperature reaction
CuS covellite

ABSTRACT

Room-temperature sulfidation of 100 nm-sized copper nanoparticles with powderous elemental sulfur in chloroform results in fast formation of irregular nanostructured CuS (covellite) particles containing nanoplates. These were characterized by Raman and UV-Vis spectroscopy, X-ray diffraction and scanning and transmission electron microscopy. The reaction is judged to occur via breakdown of the Cu nanoparticles by reactively interacting sulfur solutes and via growth of the CuS nanobodies involving interdiffusion and redox reaction of S and Cu atoms.

1. Introduction

Copper sulfides occur in a variety of compositions and morphologies [1] and are of interest for their applications in solar cells, electroconducting electrodes, optical filters, superionic materials and chemical sensors [2–7]. Various nanoparticles (plates, tubes, wires, spheres and architectures) of these binary compounds have been prepared by several techniques, e.g. room-temperature gas-solid reaction between H_2S/O_2 and Cu foils [8–10], high-temperature gas-solid reactions between Cu nanoparticles or CuCl nanorods and H_2S [11,12] or between gaseous sulfur and CuCl/Si [13] or Cu films [14], solid-liquid reactions in solution of nano-Cu_2O and thiourea [15] or thioacetamide [16], Cu nanowires and thiourea [17] and between $CuCl_2$/Na_2S and liquid surfactant [18] and many inorganic reactions in solution as solvothermal [1,19–24]), hydrothermal [25–29], microwave-induced solvothermal [30,31], ionic liquid-assisted [32], electrochemical [33], sonochemical [34,35] and γ-radiation-assisted [36] route.

The reactions of CuCl nanorods or Cu nanoparticles with gaseous H_2S [11,12], reaction of Cu_2O nanoparticles [15,16], $Cu(OH)_2$ nanoribbons [35] or Cu nanowires [18] with thiourea or thioacetamide, or reaction of spherical (colloidal) Cu nanoparticles with elemental sulfur [37] taking place in the liquid phase are interesting examples of synthesis of nano-copper sulfides from other nano-objects and belong among the sacrificial reactions of the whole nanobodies. These reactions have been studied much less than those occurring on the nanobodies surface (nanocatalysis).

As for the reaction between Cu nanoparticles and sulfur [37], this direct synthesis of CuS has been reported at 200 °C. It is also known that the reaction between bulk Cu and S is feasible at high temperatures [38,39]; it is hampered below 150 °C by the passivation effect of the CuS_x layer on copper surface, and is extremely slow at room-temperature when resulting in thin Cu_2S overgrowth on Cu with sulfur vapor exposures of the order of 10^{-7} Torr h [40].

It was in our interest to examine whether the reaction between Cu nanoparticles and sulfur can be induced at room-temperature. Here we report on a fast room-temperature reaction of Cu nanoparticles with environmentally friendly sulfur powder in chloroform leading to

* Corresponding author.
E-mail address: pola@icpf.cas.cz (J. Pola).

1631-0748/$ – see front matter
doi:10.1016/j.crci.2012.03.014

platelets containing CuS nanoparticles and propose mechanism of this reaction based on the observed morphology of the product.

2. Experimental

A single-pot reaction between sublimed sulfur powder (Lachema) and copper nanopowder (100 nm, 99.8% purity, Aldrich) in chloroform (2 ml, Riedel-deHaën for HPLC, better than 99.8%) under Ar blanket was carried out by homogenizing the suspension through magnetic stirring or immersion in ultrasonic bath for 30 min. The used amounts of Cu nanopowder (0.30 g) and sulfur powder (0.15 g) corresponded to 1:1 atomic mass ratio, and the 30-min reaction time was sufficient for an almost complete reaction. (In fact, no residual Cu and only few percent of residual S were detected by electron diffraction analyses of the solid product.) Thereafter, chloroform was evaporated and the obtained solid dark ultrafine powder was dried under low pressure and analyzed on a Nicolet Almega XR Raman spectrometer (resolution 2 cm^{-1}, excitation wavelength 473 nm and power 10 mW), a Philips XL30 CP scanning electron microscope equipped with an energy-dispersive analyzer EDAX DX-4 of X-ray radiation and, for samples dispersed in isopropanol and applied on a carbon-coated foil mounted on Cu grid, on a Philips EM 201 transmission electron microscope. Process diffraction [41] was used to evaluate and compare measured electron diffraction patterns with an XRD diffraction database [42].

X-ray diffraction patterns were collected using a PANalytical ŕPert PRO diffractometer equipped with a conventional X-ray tube ($Cu_{K\alpha}$ 40 kV, 30 mA, a line focus) in transmission mode. An elliptic focusing mirror, a divergence slit of 0.5°, an anti-scatter slit of 0.5°, a mask of 20 mm and a Soller slit of 0.02 rad were used in the primary beam. A fast linear position sensitive detector PIXcel with an antiscatter shield and a Soller slit of 0.02 rad were used in the diffracted beam. All patterns were collected in the range of 5° to 88° 2θ with a step of 0.013° and 500 sec/step.

Qualitative analysis was performed with HighScorePlus software package (PANalytical, the Netherlands, version 3.0d), Diffrac-Plus software package (Bruker AXS, Germany, version 8.0) and JCPDS PDF-2 database [43]. For quantitative analysis of XRD patterns we used Diffrac-Plus Topas (Bruker AXS, Germany, version 4.2) with structural models based on ICSD database [44]. This program permits to estimate the weight fractions of crystalline phases by means of the Rietveld refinement procedure. For estimating the amorphous content the addition of an internal standard was used. We used a known amount of zinc oxide (Sigma-Aldrich, 99.99%, fired at 700 °C for 5 hours) mixed with the sample in an agate mortar under cyclohexane.

The UV-Vis absorption spectra of the product (6.24 mg, corresponding to 0.065 mmol for CuS) and stoichiometric amounts of sulfur powder (0.39 mg, corresponding to 0.0015 mmol of S_8) and Cu nanoparticles (0.012 mmol) suspended in spectrometric grade 1-propanol (10 ml, Sigma-Aldrich) were recorded in a suprasil precision cell (1 cm pathlength) on a UV-1601 UV-Vis Shimadzu spectrophotometer.

Copper(II) oxide nanopowder (< 50 nm, Aldrich) was used as a standard for Raman spectroscopy measurements.

3. Results and discussion

The simple reaction between 100 nm-sized copper particles and elemental sulfur (cyclooctasulfur, suspended and partly soluble in chloroform) was homogenized by 30-min stirring or sonication and yielded a dark ultrafine powder. This short time of contact of the Cu and S powder used in 1:1 atomic mass ratio was sufficient for completing the reaction, as virtually no residual Cu and only few percent of residual S were detected by electron diffraction analysis of the solid product. The resulting powder was determined as a mostly crystalline material composed of covellite (a far main product) containing virtually no copper and very low amounts of sulfur, antlerite ($Cu_3(SO_4)(OH)_4$) and chalcantite ($CuSO_4.5H_2O$). Identification and characterization of the produced powder are given below.

Scanning electron microscopy (SEM) images of the powder (Fig. 1) reveal irregularly shaped particles along with variously positioned platelets with the plate size of less than 1 up to 2 μm and thickness of ca. 100 nm.

Raman spectra of the powder and reactants are compared in Fig. 2. The spectrum of the powder (Fig. 2a)

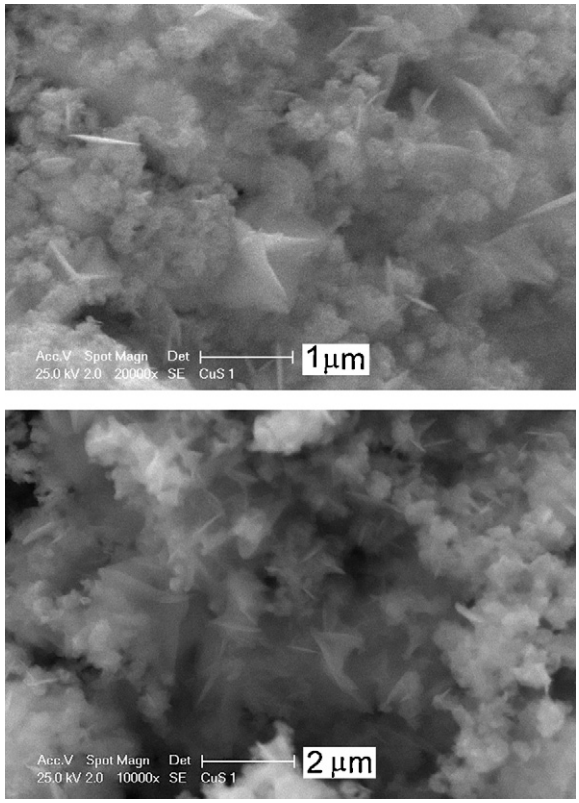

Fig. 1. Scanning electron microscopy (SEM) images showing morphology of two representative regions of the solid product with irregularly shaped particles and differently positioned nanoplates.

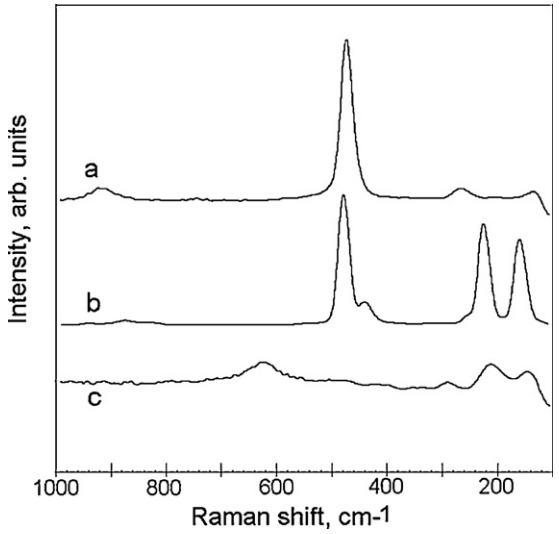

Fig. 2. Raman spectrum of the product (a), sulfur powder (b) and copper nanopowder exposed to air for 1 h (c).

shows a sharp and intense peak at 474 cm^{-1} and minor peaks at 265 and 920 cm^{-1}; the two former correspond [45–47] to S-S stretch and a lattice mode in a stoichiometric copper sulfide CuS (covellite) and the latter (found in covellite mineral [44]) was tentatively assigned [47] to the overtone of the S-S stretch mode. This spectrum includes neither peaks at 480, 225 and 134 cm^{-1} characteristic [48] of elemental cyclooctasulfur (Fig. 2b), nor those at 625 and 213 cm^{-1} assignable [49] to copper oxides. The peaks at 625 and 213 cm^{-1} observed for the 100 nm-sized Cu nanoparticles exposed for 1 h to air (Fig. 2c) illustrate the known feasible oxidation of Cu nanoparticles [37,50]. However, no Raman signature of copper oxides was observed in the spectrum of the product (Fig. 2a). Given that a minor (superficial) oxidation of the 100 nm Cu particles could take place within a short (few second)

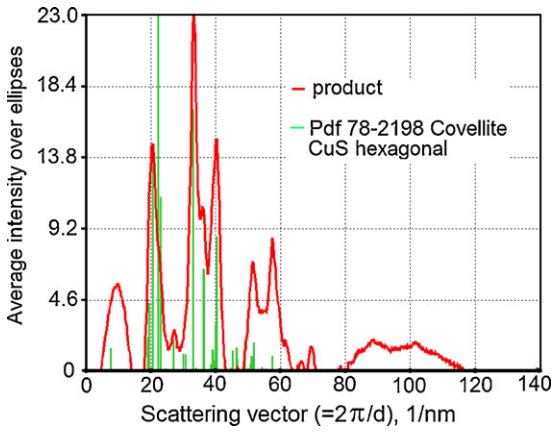

Fig. 3. Electron diffraction pattern of the product.

transfer to the reaction (sulfur in chloroform) phase, the absence of the CuO signals is due to a low detection limit or high reactivity of Cu oxides towards sulfur solutes.

The structure of CuS covellite was also proven by the pattern of electron diffraction (Fig. 3). Scrutiny of a number of samples showed a best fit to covellite Pdf 78-2198 but not to copper oxides and sulfur polymorphs. (Some similarity is only observed for sulfur unknown sample Pdf 24-1251).

The more detailed XRD analysis of the powder (Fig. 4) reveals covellite CuS (a major product) along with low quantities of unreacted sulfur, and low amounts of copper sulphates ($Cu_3(SO_4)(OH)_4$ (antlerite) and $CuSO_4.5H_2O$ (chalcantite). The estimation of amorphous content by means of an internal standard using the Rietveld method revealed an approximate value of only 10 wt. % and confirmed that the crystalline phase is in large excess.

Transmission electron microscopy (TEM) images of the powder product and of the initial Cu nanopowder are compared in Fig. 5, where ultrasonically dispersed Cu nanoparticles are shown to be agglomerated into ca. 200

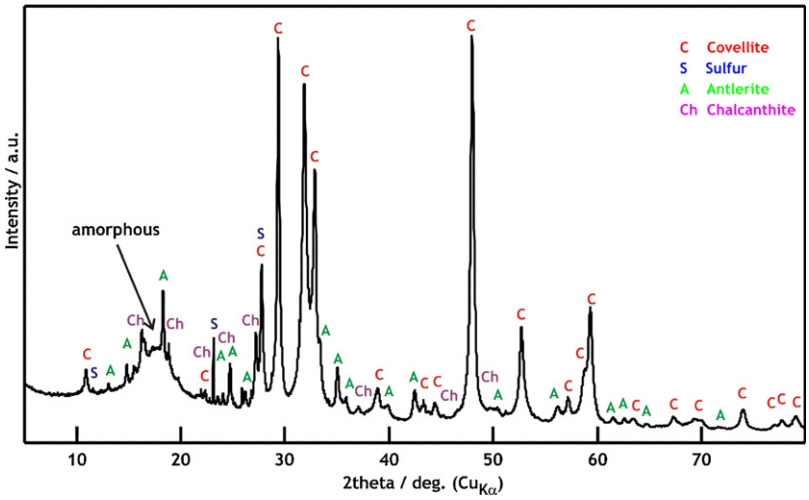

Fig. 4. XRD pattern of the product and assignment. C: Covellite (CuS), S: Sulfur (S_8); A: Antlerite ($Cu_3(SO_4)(OH)_4$); Ch: Chalcanthite ($CuSO_4.5H_2O$), a broad "hump" at about 18° 2θ corresponds to an amorphous content.

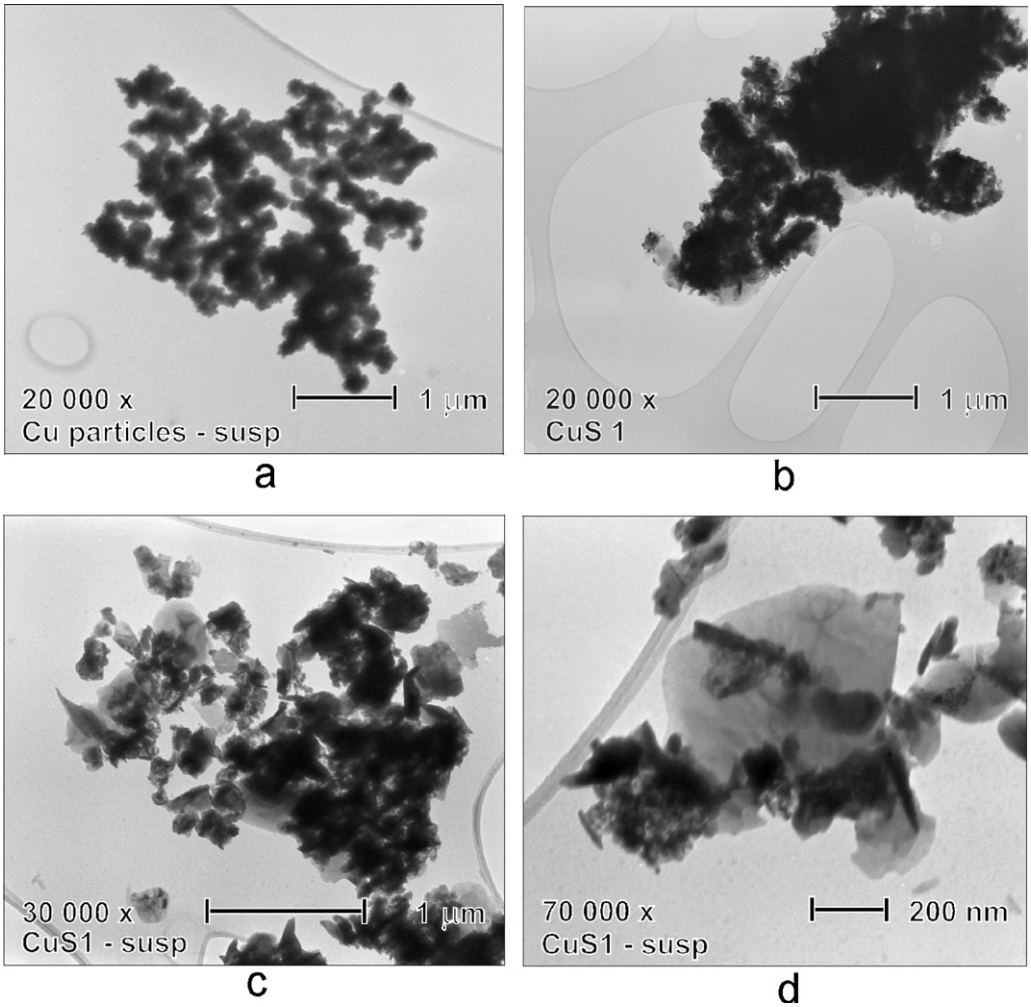

Fig. 5. Transmission electron microscopy (TEM) images of agglomerated Cu (initial) nanoparticles (a) and as obtained (b) and ultrasonically dispersed (c,d) product.

nm-sized bodies (Fig. 5a) and the powder product is shown to consist of several μm-large objects (Fig. 5b) which take upon sonication apart to smaller, ca. 200 nm up to 1 μm-sized fragments which have irregular and plate-like structure (Figs. 5c,d).

A closer inspection of TEM images revealed single crystalline plates exhibiting narrow black bands assignable to perpendicularly and at different angles standing smaller platelets whose thickness reaches 20–50 nm (Figs. 6a,b). We suggest that these variously thick platelets grow from the initial plate and coalesce in between as in the black region (Fig. 6c). The two types of the observed CuS nanoparticles – structured nanoplates and irregular nanoparticles – can then, respectively, relate to an early and later stage of the particle growth and agglomerization.

UV-Vis absorption spectra of the powder and both reactants (sulfur powder and Cu nanoparticles) dispersed in 1-propanol are compared in Fig. 7. It is shown that the spectrum of the product exhibits characteristic absorption in the range of 400–1100 nm, which corresponds [3,51] to covellite phase and resembles spectra of variously shaped nanostructures and nanoplates of CuS [21,28,32,52–54]. The observed absorption edge at ca. 690 nm is red-shifted as compared to values observed with smaller (several nm-sized) CuS nanofeatures.

The above properties indicate that the room-temperature reaction between the agglomerated 100 nm-sized Cu nanoparticles and elemental sulfur results mostly in a growth of crystalline irregularly shaped and plate-like CuS particles. The magnitude of both features exceeds 100 nm, but the plates thickness does not exceed that of the parent Cu nanoparticles. The formation of the plates indicates two-dimensional growth and can be accounted for by two possible mechanisms, either by a reaction of in-plane associated Cu nanoparticles with sulfur, or by a reactive Cu nanoparticles fragmentation and CuS growth from fragments. The second route is more probable and we presume that the Cu + S reaction is initiated after disruption of solvation shell around soluble [55] S_8 molecules, proceeds through a direct contact between S_8 and Cu nanoparticles, and leads to stoichiometric CuS via interdiffusion and redox reactions of Cu and S [56]. We assume that that the

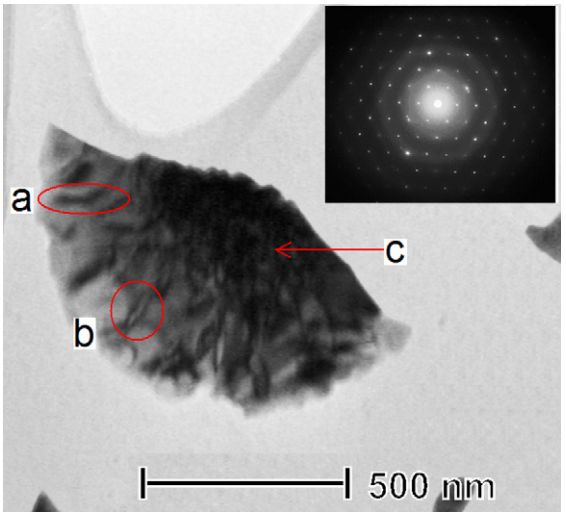

Fig. 6. Transmission electron microscopy (TEM) image and selected area electron diffraction of a single crystalline plate of the solid product. (a and b denote platelets of different thickness and c relates to a thicker region were platelets presumably merged.)

mutual diffusion of S and Cu counterparts and formation of Cu-S phase initially results in amorphous and later in crystalline state after the proper Cu/S ratio has been attained.

The formation of both ($Cu_3(SO_4)(OH)_4$) and ($CuSO_4.5H_2O$) sulphates is worthy of comment. Our measures taken to avoid contact of the Cu nanoparticles with the atmosphere were not as efficient as those used in the synthesis of CuS nanoparticles from in situ formed Cu colloid [37] and it was mainly through the unique approach in this work (and also in [50]) that oxidation of Cu nanoparticles was recognized as a very fast and size dependent reaction. It is therefore possible that the 100 nm-sized Cu nanoparticles used in our work were partly superficially oxidized and that the partial CuO_x ($x = 1,2$) cover over of the agglomerated 100 nm-sized Cu particles participated in reaction with sulfur solutes. We therefore assume that the observed (nano) sulphates were produced via a sequence of three reactions:

- a reaction between sulfur and CuO_x leading to Cu and sulfur oxides;
- a reaction between sulfur oxides and CuO to yield Cu sulphates;
- hydration of Cu suphates upon the contact to air.

The former reaction is obviously enhanced by large surface of and/or crystal defects in the nanosized and CuO_x reactants, since it normally occur [57,58], only at elevated temperatures. Such explanation involving intermediary occurrence of nanoscopic copper oxide is in accordance with no detection of copper oxides by the Raman spectra and diffraction analyses of the product.

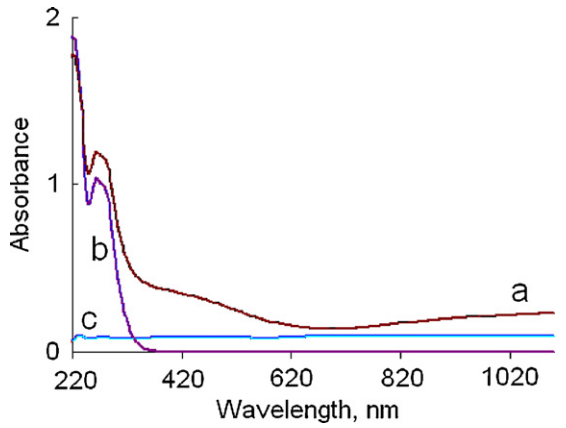

Fig. 7. UV-Vis spectra of the solid product (a), sulfur powder (b) and Cu nanoparticles (c) suspended in 1-propanol.

More study on the reactivity of Cu and other metal nanoparticles towards elemental chalcogenes in ambient atmosphere is in progress.

4. Conclusion

The reaction between agglomerated 100 nm-sized copper nanoparticles and powderous elemental sulfur in chloroform results in fast formation of irregular and plate-like nanoparticles of CuS (covellite), which are judged to grow from fragmentation of Cu nanoparticles reactively interacting with sulfur solutes.

This room-temperature formation of nanosized CuS from environmentally friendly elements may find more interest in syntheses of inorganic compounds that have yet been produced only from hazardous chemicals.

Acknowledgement

The authors thank the Grant Agency of the Czech Republic (grant n° 203/09/0931) for support.

References

[1] X. Jiang, Y. Xie, J. Lu, W. He, L. Zhu, Y. Qian, J Mater Chem 10 (2000) 2193, and refs therein.
[2] S.B. Gadgil, R. Thangaraj, O.P. Agnihotri, Thin Solid Films 145 (1986) 197.
[3] I. Gozdanov, M. Najdoski, Solid State Che 114 (1995) 469.
[4] J.S. Chung, H.J. Sohn, J Power Sources 108 (2002) 226.
[5] A.A. Sagade, R. Sharma, Chemical 133 (2008) 135.
[6] H. Lee, S.W. Yoon, J. Kim, J. Park, Nano Lett 7 (2007) 778.
[7] Y. Wu, C. Wadia, B. Sadtler, A.P. Alivisatos, Nano Lett 8 (2008) 2551.
[8] W. Zhang, S. Yang, Acc Chem Res 42 (2009) 1617.
[9] S. Wang, S. Yang, Chem Mater 13 (2001) 4794.
[10] Y. Lim, Y.-W. Ok, S.-J. Tark, Y. Kang, D. Kim, Curr Appl Phys 9 (2009) 890.
[11] Q. Wang, J.-X. Li, G.-D. Li, X.-J. Cao, K.-J. Wang, J.-S. Chen, J Cryst Growth 299 (2007) 386.
[12] C.E. Kliewer, S.L. Soled, S. Miseo, W.R. Kliewer, Microsc Microanal (12 Suppl.) (2006) 816.
[13] H.-X. Zhang, J.-P. Ge, Y.-D. Li, J Phys Chem 110 (2006) 14107.
[14] K.-J. Wang, G.-D. Li, J.-X. Li, Q. Wang, J.-S. Chen, Cryst Growth Design 7 (2007) 2265.
[15] H. Xu, W. Wang, W. Zhu, L. Zhou, Nanotechnology 17 (2006) 3649.
[16] H. Zhu, J. Wang, Inorg Chem 48 (2009) 7099.
[17] C. Wu, S.-H. Yu, S. Chen, G. Liu, B. Liu, J Mater Chem 16 (2006) 3326.
[18] W. Wang, L. Ao, Mater Chem Phys 109 (2008) 77.
[19] A. Ghezelbash, B. Korgel, Langmuir 21 (2005) 9451.
[20] W. Du, X. Qian, X. Ma, Q. Gong, H. Cao, J. Yin, Chem Eur J 13 (2007) 3241.
[21] F. Li, T. Kong, W. Bi, D. Li, Z. Li, X. Huang, Appl Surf Sci 255 (2009) 6285.

[22] S. Li, H.Z. Wang, W.W. Xu, H.L. Si, X.J. Tao, S. Lou, Z. Du, L.S. Li, J Colloid Interface Sci 330 (2009) 483.
[23] X. Dong, D. Potter, C. Erkey, Ind Eng Chem Res 41 (2002) 4489.
[24] H. Wu, W. Chen, Nanoscale 3 (2011) 5096.
[25] P. Zhang, L. Gao, J Mater Chem 13 (2003) 2007.
[26] Q. Lu, F. Gao, D. Zhao, Nano Lett 2 (2002) 725.
[27] T. Thongtem, A. Phuruangrat, S. Thongtem, Curr Appl Phys 9 (2009) 195.
[28] H. Ji, J. Cao, J. Feng, X. Chang, X. Ma, J. Liu, M. Zheng, Mater Lett 59 (2005) 3169.
[29] Z. Cheng, S. Wang, D. Si, B. Geng, J Alloys Compd 492 (2010) L44.
[30] T. Thongtem, A. Phuruangrat, S. Thongtem, J Mater Sci 42 (2007) 9316.
[31] Y. Zhang, Z.-P. Qiao, X.-M. Chen, J Solid State Chem 167 (2002) 249.
[32] L. Wang, C. Xu, D. Zhou, H. Luo, T. Ying, Bull Mater Sci 31 (2008) 931.
[33] Y.J. Yang, S. Hu, J Solid State Electrochem 12 (2008) 1405.
[34] H. Wang, J.-R. Zhang, X.-N. Zhao, S. Xu, J.-J. Zhu, Mater Lett 55 (2002) 253.
[35] H. Xu, W. Wang, W. Zhu, Mater Lett 60 (2006) 2203.
[36] Z.P. Qiao, Y. Xie, J.G. Xu, Y.J. Zhu, Y.T. Qian, J Colloid Interface Sci 214 (1999) 459.
[37] G.H. Cheng, A.R. Walker, Anal Bioanal Chem 396 (2010) 1057.
[38] R. Blachnik, A. Müller, Thermochim Acta 361 (2000) 31, and refs therein.
[39] R. Blachnik, A. Müller, Thermochim Acta 366 (2001) 47, and refs therein.
[40] O.J Cain, R.W. Vook, Thin Solid Films 58 (1979) 209.
[41] J.I. Lábár, in: L. Frank, F. Ciampor (Eds.), Proceedings of EUREM 12, Czechoslovak Society for Electron Microscopy, Brno, Czech Republic, 2000, 1379 p.
[42] Bede ZDS, version 4.0, Bede, Inc., Durham, UK, 2000.
[43] JCPDS PDF-2 database, International Centre for Diffraction Data, Newtown Square, PA, U.S.A. Release 54, 2004.
[44] ICSD database FIZ Karlsruhe, Germany, release 2011/1, 2011.
[45] S.Y. Wang, W. Wang, Z.H. Lu, Mater Sci Eng B 103 (2003) 184.
[46] C.G. Munce, G.K. Parker, S.A. Holt, G.A. Hope, Physicochem Eng Aspects 295 (2007) 152, and refs therein.
[47] B. Minceva-Sukarova, M. Najdoski, I. Grozdanov, C.J. Chunnilall, J Mol Struct 410–411 (1997) 267.
[48] B. Meyer, Chem Rev 76 (1976) 367.
[49] M. Serghini-Idrissi, M.C. Bernard, F.Z. Harrif, S. Joiret, K. Rahmouni, A. Srhiri, H. Takenouti, V. Vivier, M. Ziani, Electrochim Acta 50 (2005) 4699.
[50] M. Yin, C.K. Wu, Y.B. Lou, C. Burda, J.T. Koberstein, Y.M. Zhu, S. O'Brien, J Am Chem Soc 127 (2005) 9506.
[51] M. Kundu, T. Hasegawa, K. Terabe, K. Yamamoto, M. Aono, Sci Technol Adv Mater 9 (2008) 035011.
[52] S.K. Haram, A.R. Mahadeshwar, S.G. Dixit, J Phys Chem 100 (1996) 5868.
[53] J. Zhang, Z. Zhang, Mater Lett 62 (2008) 2279.
[54] S. Xu, Q. Wang, J. Chen, Q. Meng, Y. Jiao, Powder Technol 190 (2010) 139.
[55] R. Steudel, B. Eckert, Top Curr Chem 230 (2003) (Part of Elemental Sulfur and Sulfur-Rich Compounds, ed. R. Steudel Springer-Verlag, Berlin Vol. 1).
[56] M.V. Artemyev, V.S. Gurin, K.V. Yumashev, P.V. Prokoshin, A.M. Maljarevich, J Appl Phys 80 (1996) 7028.
[57] S.R. Satyanarayana, A.R.V.Z. Murthy, Anorg Allg Chem 330 (1964) 245.
[58] A.R.V. Murthy, Nature (London) 193 (1962) 773.